JOURNAL OF OPTOELECTRONİCS AND ADVANCED MATERİALS Vol. 9, No. 7, July 2007, p. 2180 - 2185

The determination of the optical band and optical constants of non-crystalline and crystalline ZnO thin films deposited by spray pyrolysis

F. YAKUPHANOGLU[a], S. ILICAN[b], M. CAGLAR[b], Y. CAGLAR[b,*]
[a]*Firat University, Faculty of Arts and Sciences, Department of Physics, 23169 Elazig, Turkey*
[b]*Anadolu University, Faculty of Sciences, Department of Physics, 26470 Eskisehir, Turkey*

The optical constants and optical band gaps of the non-crystalline and crystalline zinc oxide (ZnO) thin films deposited by the spray pyrolysis method onto glass substrates at the different deposition times have been investigated by optical characterization method. The structure of the films was analyzed by X-ray diffraction and the results obtained showed that the film structure changed from non-crystalline to crystalline with increasing the deposition time. The effect of film thickness on the bandgap and optical constants (refractive index, extinction coefficient and dielectric constants) of these films has been investigated and the film thickness changes the optical constants and Urbach energy values of the films. The direct band gaps E_{gi} of S1, S2, S3 and S4 thin films were determined 3.295 eV 3.280 eV, 3.297 eV and 3.295 eV, respectively. It can be evaluated that the film thickness does almost not change the optical band gap of the films. The width of the tails of localized states in the optical band gap of the films increases with increasing non crystalline film thickness. The dispersion curves of the refractive index of the non crystalline films obey single-oscillator model, whereas the curves of the crystalline films do not obey this model. The dispersion parameters such as E_o (single-oscillator energy) and E_d (dispersive energy) of the non crystalline films were determined. These values increase with increasing film thickness.

(Received March 28, 2007; accepted June 27, 2007)

***Keywords**:* Non-crystalline films, Zinc oxide, Spray Pyrolysis, X-ray diffraction, Optical properties

1. Introduction

Zinc oxide (ZnO) thin films are being extensively studied due to their interesting electro-optical properties, high electro-chemical stability, a large band gap (between 3.2 and 3.4eV at room temperature), abundance in nature and absence of toxicity. ZnO has wide range of technological applications as sensors [1, 2], heat mirrors [3], transparent electrodes [4], solar cells [5-7] and piezoelectric devices [8].

These films can be deposited by several techniques including, sputtering [9], metal organic chemical vapour deposition [10], sol gel [11] and spray pyrolysis [12, 13]. Among these, the spray pyrolysis method has the advantages of low cost, easy-to-use, safe, and can be implemented in a standard laboratory.

Accurate knowledge of the absorption coefficient, optical band gap and refractive index of semiconductors is indispensable for the design and analysis of various optical and optoelectronic devices. It is possible to determine indirect and direct transition occurring in band gap of the materials by optical absorption spectra. The data transmittance can be analyzed to determine optical constants such as refractive index, extinction coefficient and dielectric constant.

There have been extensive studies on the crystalline structure and optical transmittance of ZnO thin films. There are, however, few studies on the optical constants of crystalline and non-crystalline ZnO thin films. In this work, we deposited non-crystalline and crystalline ZnO thin films successfully onto glass substrate. We also investigate the role of the film thickness and deposition time on the optical properties (the band gap, optical constants such as refractive index, extinction coefficient and dielectric constant, the Urbach energy and the dispersion parameters such as single-oscillator energy and dispersive energy).

2. Experimental

The spray pyrolysis method used here is basically a chemical deposition method in which fine droplets of the desired material are sprayed onto a heated substrate. Continuous films are formed on the hot substrate by thermal decomposition of the material droplets.

The ZnO films were deposited onto glass slices, chemically cleaned, using the spray pyrolysis method at 475 ^{o}C substrate temperature. 0.2M solution of zinc acetate dehydrate ($Zn(CH_3COO)_2.2H_2O$) diluted in methanol and deionized water (3:1) was used for all the films. A few drops of acetic acid were added to improve the clarity of solution. Nitrogen was used as the carrier gas, pressure at 0.2 kgcm^{-2}. The ultrasonic nozzle to substrate distance was 30 cm and during deposition, solution flow rate was held constant at 4mlmin^{-1}. The substrate temperature was measured using an Iron-Constantan thermocouple. The thickness of the thin films was measured by weight difference method using a sensitive microbalance.

The structural analysis of all the thin films was performed with a RIGAKU RINT 2000 Series X-Ray Automatic Diffractometer with CuK$_\alpha$ (λ=1,54059Å)

radiation. The diffractometer reflections were taken at room temperature and the value of 2θ were swapped between 20° and 70° with a scanning speed of 0.02°/s at 40 kV and 30 mA.

The optical measurements of ZnO films were carried out at room temperature using Shimadzu UV-VIS-2450 scanning spectrophotometer in the wavelength range from 190 to 1100 nm. The substrate absorption is corrected by introducing an uncoated cleaned glass substrate in the reference beam.

3. Results and discussion

3.1. Film formation

When aerosol droplets arrive close to the heated substrates, a pyrolytic process occurs and highly adherent ZnO films were produced. Possible reaction proposed by Paraguay et al. is as follows [14]

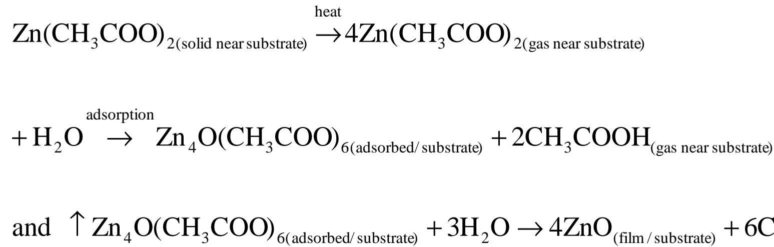

$$Zn(CH_3COO)_{2(\text{solid near substrate})} \xrightarrow{\text{heat}} 4Zn(CH_3COO)_{2(\text{gas near substrate})}$$

$$+H_2O \xrightarrow{\text{adsorption}} Zn_4O(CH_3COO)_{6(\text{adsorbed/substrate})} + 2CH_3COOH_{(\text{gas near substrate})}$$

$$\text{and } \uparrow Zn_4O(CH_3COO)_{6(\text{adsorbed/substrate})} + 3H_2O \rightarrow 4ZnO_{(\text{film/substrate})} + 6CH_3COOH_{(\text{gas})} \uparrow$$

3.2. Structural properties

The crystal structure and orientation of the ZnO thin films were investigated by X-ray diffraction (XRD) patterns. Fig. 1(a) shows the diffraction patterns of ZnO thin films deposited at deposition time=5min with different thickness. These films, i.e., 87 nm and 107 nm were named as S1 and S2, respectively. XRD patterns indicate that the films with low deposition time are almost non-crystalline phase, whereas at the deposition time=10min, the films are transformed to polycrystalline phase [15], as shown in Fig. 1(b). The ZnO films deposited at deposition time =10 min with different thickness i.e., 318 nm and 346 nm were named as S3 and S4, respectively.

As shown in Fig. 1(b), the S1 and S2 films have (101) as the preferred orientation. Another major orientation present is (002), while other orientations like (100), (102), (110), (103) and (112), are also seen with comparatively lower intensities.

The relative percentage error for the observed and JCPDS standard d-values for crystalline ZnO thin films are calculated using the formula [16]

$$\text{Relative percentage error} = \frac{|Z_H - Z|}{Z} \text{x}100 \quad (1)$$

where Z_H represents the actual d value obtained and Z is the standard d value in JCPDS card file. 2θ, d-values, and d% error data calculated by using equation (1) are given in Table 1 for the crystalline ZnO thin films. The average relative percentage error is found to be 0.03% and 0.22% for S3 and S4 films, respectively. The experimental d-values and JCPDS d-values are in relatively good agreement [15].

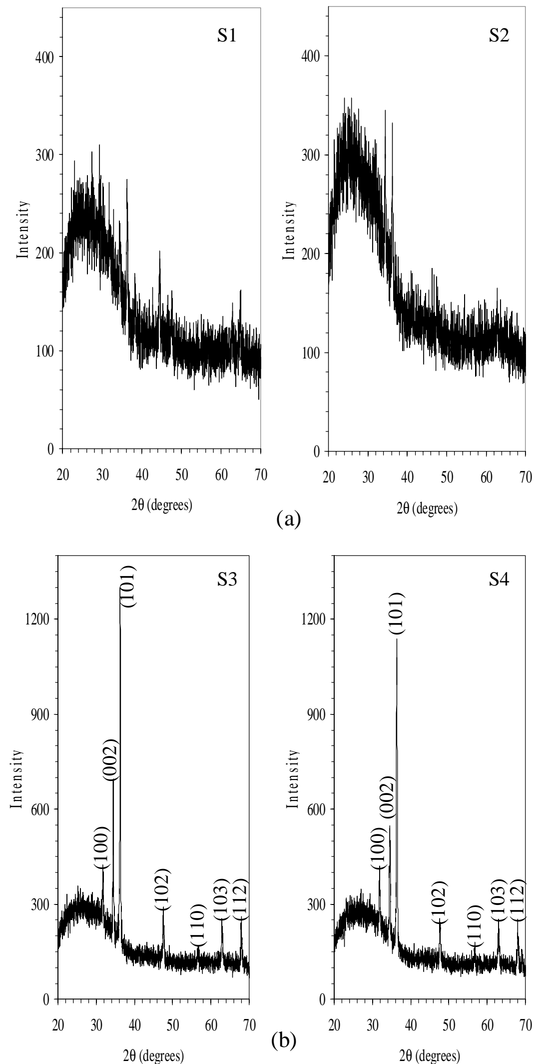

Fig. 1. X-ray diffraction spectra of non-crystalline and crystalline ZnO thin films.

Table 1. The X-ray diffraction data results of the crystalline ZnO thin films.

	S3					S4				
(hkl)	2θ	d(Å)	d% error	I/Io	TC(hkl)	2θ	d(Å)	d% error	I/Io	TC(hkl)
(100)	31.799	2.8118	0.11	15.2	0.5200	31.899	2.8032	0.39	19.8	0.6784
(002)	34.460	2.6005	0.10	44.2	1.5122	34.580	2.5918	0.44	36.1	1.2369
(101)	36.241	2.4767	0.03	100	3.4213	36.360	2.4688	0.29	100	3.4263
(102)	47.522	1.9118	0.04	14.3	0.4893	47.640	1.9073	0.20	14	0.4797
(110)	56.542	1.6263	0.17	4.4	0.1506	56.662	1.6232	0.09	6.8	0.2329
(103)	62.839	1.4777	0.04	12.9	0.4413	62.939	1.4755	0.11	14.2	0.4865
(112)	67.881	1.3796	0.10	13.6	0.4653	67.962	1.3782	0	13.4	0.4591

The lattice constants for hexagonal ZnO film are reported in JCPDS standard data a=3.24982 Å and c=5.20661 Å [15]. The analytical method [17] for calculating lattice constants is used to calculate a and c for the crystalline ZnO thin films, where it was found that for the S3 film a=3.24598 Å and c=5.20100 Å, S4 film a=3.23686Å and c=5.18360 Å. These calculated values are agreement with JCPDS data.

The grain size of crystallites was calculated using a well-known Scherrer's formula [17]:

$$D = \frac{0.9\lambda}{\beta \cos\theta} \quad (2)$$

where D is the grain size of crystallite, λ (=1.54059Å) the wavelength of X-rays used, β the broadening of diffraction line measured at half its maximum intensity in radians and θ the angle of diffraction.

The grain size values of the crystalline ZnO thin films are 32.34 nm and 27.77 nm for S3 and S4, respectively. It can be seen that the grain size decreases with the increasing the film thickness.

The texture coefficient (TC) represents the texture of the particular plane, deviation of which from unity implies the preferred growth. The different texture coefficient TC(hkl) have been calculated from the x-ray data using the well-known formula [18]

$$TC(hkl) = \frac{[I(hkl)/I_o(hkl)]}{\left[N^{-1}\sum_n I(hkl)/I_o(hkl)\right]} \quad (3)$$

where I(hkl) is the measured relative intensity of a plane (hkl), I_o(hkl) is the standard intensity of the plane (hkl) taken from the JCPDS data, N is the reflection number and n is the number of diffraction peaks. TC(hkl) and I/I_o values of all the films are tabulated in Table 1. It can be seen that the highest TC was in (101) plane for the S3 and S4 films.

3.3. Determination of the optical band gap and Urbach energy of the films

The most direct and perhaps the simplest method for probing the band structure of semiconductors is to measure the absorption spectrum. The transmission spectra of non-crystalline and crystalline ZnO thin films having different thickness are shown in Fig. 2.a and Fig. 2.b. The data for the non-crystalline and crystalline films shows peculiar characteristics that we will attribute to inhomogeneities in the film. The crystalline films showed interference fringes pattern in transmission spectrum. This revealed the smooth reflecting surfaces of the film and there was not much scattering loss at the surface. It is interesting to note that, the average optical transmission of both the non-crystalline and crystalline thin films which are small thickness in the visible region are higher than the others.

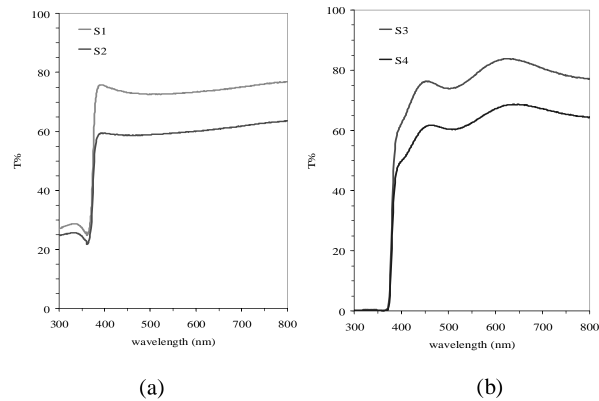

Fig. 2. Optical transmission spectra of the non-crystalline and crystalline ZnO thin films.

In order to determine the optical band gap of the films, the absorbance spectra of the films were recorded at room temperature. The absorption coefficient (α) was calculated from the absorbance spectrums using the formula:

$$\alpha(\upsilon) = 2.303(A/d) \quad (4)$$

where d is the film thickness and A is the optical absorbance. The optical absorption edge was analyzed by the following equation [19],

$$\alpha h\upsilon = A(h\upsilon - E_g)^m \quad (5)$$

where A is a constant, m value is respectively 1/2 and 2 for direct and indirect transitions. The variation of $(\alpha h\upsilon)^2$ with photon energy $h\upsilon$ non-crystalline and crystalline ZnO thin films is shown in Fig. 3.a and Fig.

3.b. It has been observed that the plots of $(\alpha h\upsilon)^2$ versus $h\upsilon$ are linear over a wide range of photon energies indicating the direct type of transitions. The intercepts (extrapolations) of these plots (straight lines) on the energy axis give the energy band gaps. The direct band gaps E_{gi} of S1, S2, S3 and S4 thin films were determined 3.295 eV 3.280eV, 3.297eV and 3.295eV, respectively. Because of not being sharp increasing in transmission spectra at near the absorption edge for non-crystalline ZnO thin films, indirect band gaps were also determined. So, indirect band gaps of the non-crystalline ZnO thin films were determined by Taue plot $f(h\upsilon) = (\alpha h\upsilon)^{1/2}$. It is shown the Taue plots for non-crystalline ZnO thin films in Fig. 4. The indirect band gaps of the non-crystalline thin films, S1 and S2 were determined 3.15 eV and 3.10 eV, respectively.

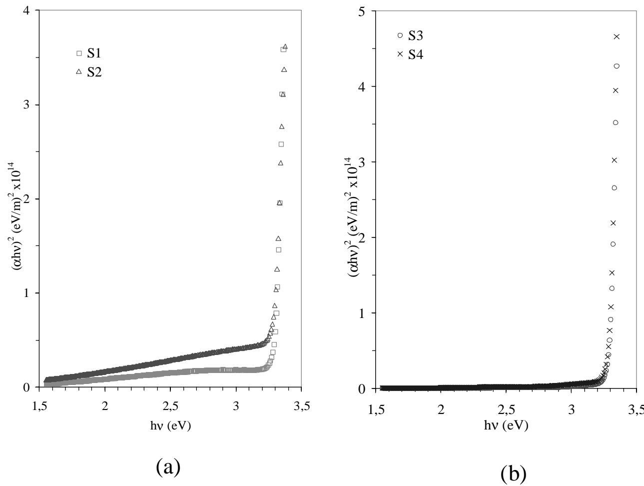

Fig. 3. The plots of $(\alpha h\upsilon)^2$ vs. photon energy of the non-crystalline and crystalline ZnO thin films.

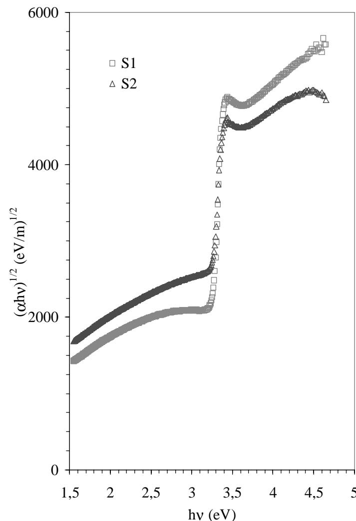

Fig. 4. Tauc plots of the non-crystalline ZnO thin films.

It is also assumed that the absorption coefficient near the band edge shows an exponential dependence on photon energy and this dependence is given as follows [20],

$$\alpha = \alpha_o \exp\left(\frac{h\upsilon}{E_u}\right) \tag{6}$$

where α_o is a constant and E_u is Urbach energy interpreted as the width of the tails of localized states, associated with the amorphous state, in the forbidden gap. The $\ln(\alpha)$ vs. photon energy plots for non-crystalline ZnO thin films are shown in Fig. 5. The values of E_u obtained from this figure are given in Table 2. It is believed that the exponential dependence of a on photon energy may arise from random fluctuations of the internal fields associated with the structural disorder in many amorphous materials. The E_u value of S1 sample is higher than that of S2 sample. This suggests that the film thickness increases the Urbach energy referred the width of the band tail. This is probably due to the structural disorders in the samples.

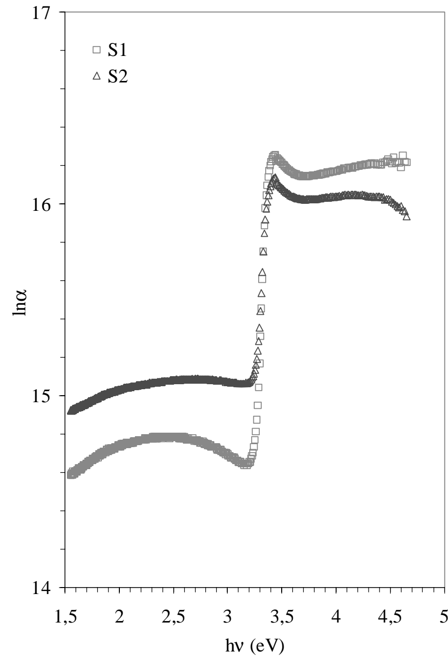

Fig. 5. The Urbach plots of the non-crystalline ZnO thin films.

3.4. The dispersion of the refractive index of the films

The refractive index of the samples can be obtained from the following equation [21],

$$n = \left(\frac{1+R}{1-R}\right) + \sqrt{\frac{4R}{(1-R)^2} - k^2} \tag{7}$$

where k ($k = \alpha\lambda / 4\pi$) is the extinction coefficient. The refractive index values were calculated by using equation (6). The variation of the refractive index and the extinction coefficient k with photon energy for the non-crystalline thin ZnO films with different thickness is shown in Figs. 6.a and 6.b. On the other hand, if the refractive index and extinction coefficient are known, the real and imaginary parts of dielectric constant of the films can be also estimated. The real and imaginary parts of complex dielectric constant are expressed as [22],

$$\varepsilon_1 = n^2 - k^2 , \qquad \varepsilon_2 = 2nk \tag{8}$$

where ε_1 is the real part and ε_2 is the imaginary part of the dielectric constant. The dependence of the real (ε_1) and imaginary (ε_2) parts of dielectric constant on photon energy are shown in Fig. 7.a and Fig. 7.b for non-crystalline ZnO thin films with different thickness, respectively. The real and imaginary parts follow the same pattern and it is seen that the values of real part are higher than the imaginary parts.

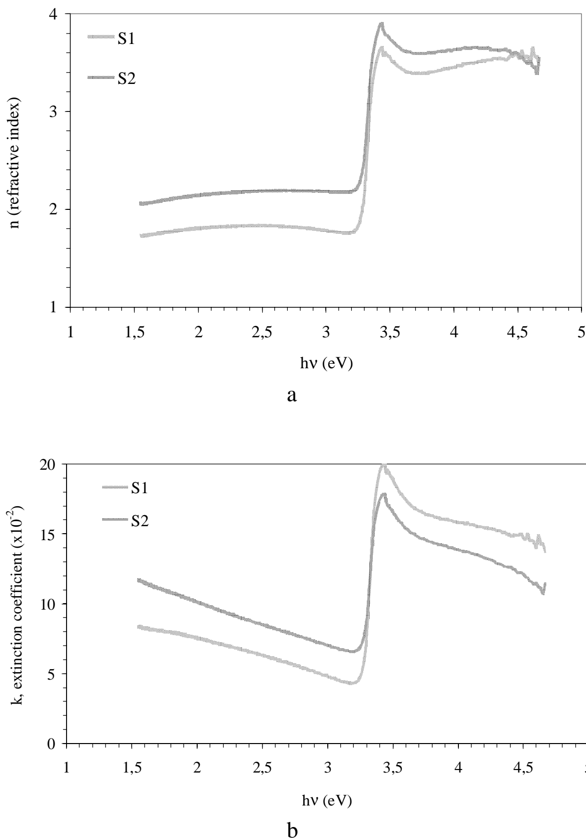

Fig. 6. The variation of refractive index and extinction coefficient of the non-crystalline ZnO thin films with photon energy. (a - refractive index; b - extinction coefficient)..

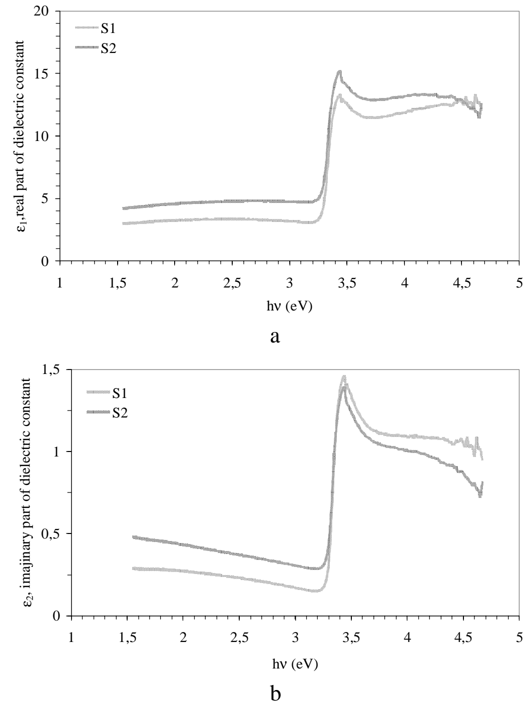

Fig. 7. The variation of real and imaginary parts of the dielectric constant of the non-crystalline ZnO thin films with photon energy.

The data on the spectral dependence of refractive index were evaluated according to the single-oscillator model proposed by Di-Domenico and Wemple [23]. The dispersion parameters of various materials (both non-crystalline and crystalline) were investigated by using this model in the literature [24-28]. This model describes the dielectric response for transitions below the optical gap. It plays an important role in determining the behaviour of the refractive index. The dispersion data of the refractive index can be described by a single-oscillator model [23]:

$$n^2 = 1 + \frac{E_d E_o}{E_o^2 - (h\nu)^2} \tag{9}$$

where E_o and E_d are single-oscillator constants. E_o is the average excitation energy for electronic transitions and E_d is the dispersion energy which is a measure of the strength of interband optical transitions. The oscillator energy E_o is an average energy gap. The dispersion curve of the refractive obeys the single oscillator model, while S3 and S4 films do not obey. Thus, the oscillator parameters were only determined for the S1 and S2 films. Fig. 8 shows plots of $(n^2-1)^{-1}$ versus $(h\upsilon)^2$ for the non-crystalline films. E_o and E_d are determined directly from the gradient, $(E_o E_d)^{-1}$ and the intercept (E_o/E_d), on the vertical axis. Also, the long wavelength refractive index (n_∞) for the non-crystalline thin films was determined from the interception of the vertical axis in Figs. 8. The values of E_o and E_d for the non-crystalline ZnO thin films are given in Table 2. These values increase with increasing of the film thickness.

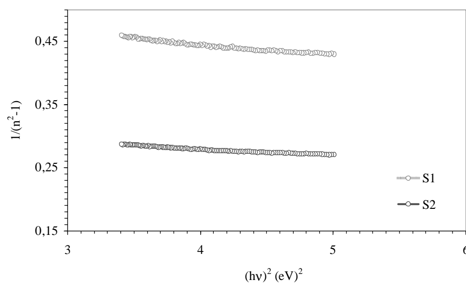

Fig. 8. Plots of $(n^2-1)^{-1}$ vs. $(h\upsilon)^2$ of the non-crystalline ZnO thin films.

Table 2. The optical band gap, Urbach energy and refractive index dispersion parameters of the non-crystalline ZnO thin films.

Film name	E_u (meV)	E_o (eV)	E_d (eV)	M_{-1}	M_{-3} $(eV)^{-2}$	n_∞
S1	121	5.36	10.36	1.93	0.067	1.71
S2	455	5.53	17.20	3.11	0.101	2.03

The M_{-1} and M_{-3} moments of the optical spectra can be obtained from the following relations

$$E_o^2 = \frac{M_{-1}}{M_{-3}}, \qquad E_d^2 = \frac{M^3_{-1}}{M_{-3}} \tag{10}$$

The obtained values are given in Table 2. It is seen that M_{-1} and M_{-3} moments increase with the increasing of the film thickness for non-crystalline films. Although M_{-1} values increase with the increasing of the film thickness for crystalline films, M_{-3} moments indicate to decrease.

4. Conclusions

The optical constants and optical band gaps of the non-crystalline and crystalline zinc oxide (ZnO) thin films deposited by the spray pyrolysis method onto glass substrates at the different deposition times have been investigated by optical characterization method. X-ray diffraction results showed that the film structure changed from non-crystalline to crystalline with increasing the deposition time. The direct band gaps E_{gi} of S1, S2, S3 and S4 thin films were determined 3.295 eV 3.280 eV, 3.297 eV and 3.295 eV, respectively. The film thickness does almost not change the direct optical band, whereas the film thickness changes the optical constants (refractive index, extinction coefficient and dielectric constants), and Urbach energy values of the films. The dispersion curves of the refractive index of the non crystalline films obey single-oscillator model, whereas the curves of the crystalline films do not obey this model. The dispersion parameters of the non crystalline films were determined and these values increase with increasing film thickness. The M_{-1} and M_{-3} optical moments of the non-crystalline films increase with the increasing film thickness.

References

[1] P. Mitra, A. P. Chatterjee, H.S. Maiti, Mater. Lett. **35**, 33 (1998).
[2] C. H. Kwon, H. K. Hong, D. H. Yun, K. Lee, S. T. Kim, Y. H. Roh, B. H. Lee, Sens. Actuators B **25**, 610 (1995).
[3] K. L. Chopra, S. Major, D. K. Pandya, Thin Solid Films **102**, 1 (1983).
[4] S. Major, A. Banerjee, K. L. Chopra, Thin Solid Films **143**, 19 (1986).
[5] J. B. Yoo, A. L. Fahrenbruch, R. H. Bube, J. Appl. Phys. **68**, 4694 (1990).
[6] D. Dimova-Malinovska, J. Lumin. **80**, 207 (1999).
[7] Z.-C. Jin, I. Hamberg, C. G. Granqvist, B. E. Sernelius, K.-F. Berggren, Thin Solid Films **164**, 381 (1988).
[8] J. G. E. Gardeniers, Z. M. Rittersma, G. J. Burger, J. Appl. Phys. **83**, 7844 (1998).
[9] Soon-Jin So, Choon-Bae Park Journal of Crystal Growth **285**, 606 (2005).
[10] S. T. Tan, B. J. Chen, X. W. Sun, X. Hu, X. H. Zhang, S. J. Chua, Journal of Crystal Growth 281, 571 (2005).
[11] Young-Sung Kim, Weon-Pil Tai, Su-Jeong Shu, Thin Solid Films **491**, 153 (2005).
[12] A. Ashour, M. A. Kaid, N. Z. El-Sayed, A. A. Ibrahim, Applied Surface Science, In Press (2005).
[13] R. Martins, R. Igreja, I. Ferreira, A. Marques, A. Pimentel, A. Gonçalves, E. Fortunato, Materials Science and Engineering B **118**, 135 (2005).
[14] D. F. Paraguay, L. W. Estrada, D. R. Acosta, M. E. Andrade, Miki Yoshida, Thin Solid Films **350**, 192 (1999).
[15] Joint Committee on Powder Diffraction Standards, Powder Diffraction File, card no: 36-1451.
[16] D. P. Padiyan, A. Marikani, Cryst. Res. Technol. **37**, 1241 (2002).
[17] B. D. Cullity, S. R. Stock, Elements of X-Ray Diffraction, Prentice Hall, 2001, 3rd ed.
[18] C. S. Barret, T. B. Massalski, Structure of Metals, Pergamon Press, Oxford,1980.
[19] N. F. Mott, R. W. Gurney, Electronic Processes in Ionic Crystals, Oxford Univ. Press, London 1940.
[20] F. Urbach, Phys Rev. **92**, 1324 (1953).
[21] S. K. J. Al-Ani, Y. Al-Ramadin, M. S. Ahmad, A. M. Zihlif, M. Volpe, M. Malineonico, E. Martuscelli, G. Ragosta, Polymer Testing, **18**, 611 (1999).
[22] E. Abd El-Wahabb, A. E. Bekheet, Applied Surface Science, **173**, 103 (2001).
[23] M. DiDomenico, S. H. Wemple, J. Appl. Phys. **40**, 720 (1969).
[24] Akram K. S. Aqili, Z. Ali, A. Maqsood, Applied Surface Science **167**, 1 (2000).
[25] A. H. Ammar, Applied Surface Science **201**, 9 (2002).
[26] F. Yakuphanoglu, A. Cukurovali, I. Yilmaz, Physica B, **353**, 210 (2004).
[27] P. K. Manoj, K. G.Gopchandran, Peter Koshy, V. K. Vaidyan, Benny Joseph, Optical Material, In Press (2005).
[28] El-Sayed M. Farg, Optics & Laser Technlogy **38**, 14 (2006).

*Corresponding author: yasemincaglar@anadolu.edu.tr